Letter

Majorana stellar representation of twisted photons

Nicolas Fabre [1,2] Andrei B. Klimov [3] Romain Murenzi [4] Jean-Pierre Gazeau [5] and Luis L. Sánchez-Soto [1,6]

[1] *Departamento de Óptica, Facultad de Física, Universidad Complutense, 28040 Madrid, Spain*
[2] *Telecom Paris, Institut Polytechnique de Paris, 91120 Palaiseau, France*
[3] *Departamento de Física, Universidad de Guadalajara, 44420 Guadalajara, Jalisco, Mexico*
[4] *The World Academy of Sciences, TWAS, ICTP, Strada Costiera 1, 34151 Trieste, Italy*
[5] *Université Paris Cité, CNRS, Astroparticule et Cosmologie, 75013 Paris, France*
[6] *Max-Planck-Institut für die Physik des Lichts, 91058 Erlangen, Germany*

(Received 17 March 2023; revised 29 May 2023; accepted 28 June 2023; published 12 July 2023)

Majorana stellar representation, which visualizes a quantum spin as points on the Bloch sphere, allows quantum mechanics to accommodate the concept of trajectory, the hallmark of classical physics. We extend this notion to the discrete cylinder, which is the phase space of the canonical pair angle and orbital angular momentum. We demonstrate that the geometrical properties of the ensuing constellations aptly encapsulate the quantumness of the state.

DOI: 10.1103/PhysRevResearch.5.L032006

Introduction. Quantum information science is the driving force for the revolutionary changes in information technology that we are witnessing today. This impressive progress is based on the observation that fundamental quantum phenomena lead to completely novel ways of encoding, processing, and transmitting information.

Thus far, most of the experiments in this field have been performed with qubits, i.e., two-level systems. A very intuitive way to represent these states and the operations performed on them is to use the Bloch sphere, which is nothing but the associated phase space. Unfortunately, for complex quantum systems involving n qubits, this simple construction does not work. There is, however, a clever strategy devised by Majorana [1] that maps symmetric n-qubit pure states as a collection of n points on the Bloch sphere. Several decades after its conception, this representation has recently attracted a great deal of attention and has been applied to numerous challenging problems, including representing many-body states [2–5], entanglement classification [6–8], Bose-Einstein condensates [9–11], polarization [12–15], structured beams [16,17], quantum metrology [18–21], and Berry phases [22–24].

Despite these impressive advances, considerable effort is underway to explore higher-dimensional quantum systems, also called qudits. Qudits have been created on various physical platforms, such as photonic systems [25,26], continuous spin systems [27,28], ion traps [29], nuclear magnetic resonance [30], and molecular magnets [31]. Yet the most popular implementation is in terms of the photonic orbital angular momentum (OAM) states [32]: These twisted photons can be used as alphabets to encode information beyond one bit per single photon, which offers great potential for quantum information tasks [33,34]. They provide a larger state space to store and process information and the ability to do multiple control operations simultaneously, which is a significant advantage for quantum computation [35]. Finally, OAM qudits have also been instrumental in analyzing various fundamental questions [36–39].

A proper description of the OAM requires dealing with its conjugate variable, the angular position. The role of angles in quantum mechanics has a long history and requires more care than might be expected [40–44]. Since the OAM has an unbounded spectrum (that includes positive and negative integers), it is possible to introduce a *bona fide* angle operator. Periodicity, however, brings out subtleties that have triggered long and heated discussions [45–47].

The phase space of this canonical pair is the discrete cylinder $\mathcal{S}_1 \times \mathbb{Z}$ [48–50]. The tools required to describe these systems in that geometric arena have been developed, including a proper Wigner function [51–55]. Coherent states for this pair have also attracted much attention [56–62]. We insist in that a satisfactory description of a physical phenomenon requires the use of a suitable phase space. Whereas the plane and the sphere are standards for the description of continuous and spin variables, the use of the cylinder is not as extended as it should be in the OAM community.

Given the relevant role played by the Majorana representation on the Bloch sphere, one might rightly ask whether that can be extended to the cylinder. The idea of constellation can be presented in a variety of ways and is related to various sound mathematical concepts [63,64]. Perhaps the most direct approach is using the overlap of coherent states with the state we want to investigate: The zeros of this quantity define the corresponding stars. We pursue this idea and work out a general method for finding stars in the discrete cylinder. Since the geometry of a constellation elegantly encapsulates all the properties of the state [65], we characterize the quantumness using the multipoles associated to the stars.

Cylinder as a phase space. As anticipated, we want to describe OAM, represented by the operator $\hat{L}$ and its conjugate variable, the angle $\hat{\phi}$. This conjugacy is usually expressed via the commutation relation $[\hat{E}, \hat{L}] = \hat{E}$, with $\hat{E} = e^{i\hat{\phi}}$, which is distinctive of the Euclidean algebra $\mathfrak{e}(2)$ [66–68]. Fortunately, a long discussion about the properties of this pair turns out to be unnecessary to settle a phase-space description. For our purposes, it is enough to introduce two conjugate bases

$$|\phi\rangle = \frac{1}{\sqrt{2\pi}} \sum_{\ell\in\mathbb{Z}} e^{-i\ell\phi}\, |\ell\rangle\,, \quad |\ell\rangle = \frac{1}{\sqrt{2\pi}} \int_0^{2\pi} d\phi\, e^{i\ell\phi}\, |\phi\rangle\,, \tag{1}$$

which are normalized according to $\langle \ell|\ell'\rangle = \delta_{\ell\ell'}$ and $\langle\phi|\phi'\rangle = \delta_{2\pi}(\phi-\phi') = \sum_{n\in\mathbb{Z}} \delta(\phi - \phi' - 2n\pi)$. One can directly check that the states $|\ell\rangle$ and $|\phi\rangle$ are precisely eigenvectors of the fundamental variables $\hat{L}\,|\ell\rangle = \ell\,|\ell\rangle$ and $\hat{E}\,|\phi\rangle = e^{i\phi}\,|\phi\rangle$, respectively. Denoting the wave-function components of a pure state $|\psi\rangle$ in both bases as $\psi_\ell = \langle\ell|\psi\rangle$ and $\psi(\phi) = \langle\phi|\psi\rangle$, they are Fourier related, which corroborates the complementarity of these variables.

Stellar representation on the cylinder. To proceed further, we need to construct coherent states for the Euclidean symmetry $\mathfrak{e}(2)$. We depart here from algebraic standard approaches, such as those due to Perelomov [69] and Barut and Girardello [70] (see also Ref. [71]), and take a different route [72], whose domain of applicability is much wider. The natural framework is the Hilbert space $L^2(X, \mu)$ of all the square integrable functions defined on the phase space X (i.e., the discrete cylinder) and μ being the associated invariant measure. On a quite general level, the problem of finding coherent states can be solved if one finds a map from X to the space of quantum states, denoted by $\mathcal{H}$, $X \ni x \mapsto |x\rangle \in \mathcal{H}$, obeying the following two conditions,

$$\langle x|x\rangle = 1, \quad \int_X d\mu(x) w(x)\, |x\rangle\, \langle x| = \mathbb{1}, \tag{2}$$

where $w(x)$ is a weight factor. The family of states $|x\rangle$ are the coherent states we are looking for. Let $\{\Upsilon_n(x)\}$ be an orthonormal set of elements of $L^2(X, \mu)$, such that $0 < \mathcal{M}(x) \equiv \sum_n |\Upsilon_n(x)|^2 < \infty$. Let $\{|e_n\rangle\}$ be an orthonormal basis of $\mathcal{H}$ and suppose that the set $\{\Upsilon_n(x)\}$ is in one-to-one correspondence with the basis $\{|e_n\rangle\}$. Then, the states

$$|x\rangle = \frac{1}{\sqrt{\mathcal{M}(x)}} \sum_n \Upsilon_n^*(x)\, |e_n\rangle \tag{3}$$

satisfy the requirements (2) with $w(x) = \mathcal{M}(x)$.

The discrete cylinder $X = \mathcal{S}_1 \times \mathbb{Z}$ is parametrized by the coordinates $x \equiv (\phi, \ell)$. The natural measure on X is $\int_X d\mu(x) = \frac{1}{2\pi} \sum_{\ell\in\mathbb{Z}} \int_0^{2\pi} d\phi$. There is no *a priori* preferred choice for the set of functions $\{\Upsilon_n\}$ and several candidates have been proposed [71], including the wrapped Gaussian [60], the Dirichlet [73] and the Fejér kernels [74], and the von Mises distribution [75]. Here, for reasons that will become clear later, we prefer the orthonormal set

$$\Upsilon_n(\phi, \ell) = \frac{e^{-\frac{1}{2}\ell^2}}{\sqrt{\varpi}} e^{-\frac{1}{2}n^2} e^{n(\ell + i\phi)}, \tag{4}$$

where the normalization constant involves the number $\varpi = \sum_{n\in\mathbb{Z}} e^{-n^2} \approx 1.776\,372$. With this choice, we have $\mathcal{M}(x) = w(x) = 1$, and our coherent states read as

$$|\phi, \ell\rangle = \frac{e^{-\frac{1}{2}\ell^2}}{\sqrt{\varpi}} \sum_{n\in\mathbb{Z}} e^{-\frac{1}{2}n^2} e^{n(\ell - i\phi)} |e_n\rangle. \tag{5}$$

The states $\{|e_n\rangle\}$ can be any orthonormal basis. For instance, for our purposes here they can be considered as Fourier exponentials $e^{in\phi}$, which are the eigenstates of $\hat{L}$ in the Hilbert space $L^2(\mathcal{S}_1)$. It is striking that, given the crucial role played by coherent states for continuous and spin variables, these states have not be exploited yet in the realm of OAM.

The coherent states are thus parametrized by the conjugate of the complex number $e^{\ell + i\phi} \equiv e^z$, which is a conformal mapping of the complex plane $\mathbb{C}$ onto the cylinder. This is the counterpart of the stereographic projection in the unit sphere, which is an essential ingredient in defining the SU(2) coherent states [69].

In terms of the set $\{\Upsilon_n(\phi, \ell)\}$ the resolution of the identity (2) holds true. This immediately suggests that to every normalized state $|\psi\rangle \in \mathcal{H}$ we can attach the normalized coherent-state wave function $\psi(\phi, \ell) = \langle\phi, \ell|\psi\rangle$, which we call its stellar representation. It is nothing but the overlap of the given state with the cylinder coherent states. Interestingly, $\psi(\phi, \ell)$ is a linear representation of $|\psi\rangle$, contrary to the Wigner function, which is quadratic in the wave function. The associated probability distribution $Q_\psi(\phi, \ell) = |\psi(\phi, \ell)|^2$ is the Husimi function [76] for the cylinder, with normalization $\frac{1}{2\pi} \sum_{\ell\in\mathbb{Z}} \int_0^{2\pi} d\phi\, Q_\psi(\phi, \ell) = 1$.

For a pure state $|\psi\rangle$, its components ψ_ℓ in the OAM basis $\{|e_\ell\rangle = |\ell\rangle\,, \ell \in \mathbb{Z}\}$ are the variables used in the laboratory to synthesize arbitrary states with spatial light modulators [77]. In terms of them, the stellar representation is written as

$$\psi(\phi, \ell) = \frac{e^{-\frac{1}{2}\ell^2}}{\sqrt{\varpi}} \sum_{\ell'\in\mathbb{Z}} e^{-\frac{1}{2}\ell'^2} \psi_{\ell'}\, e^{\ell' z} \equiv e^{-\frac{1}{2}\ell^2} \tilde{\psi}(z). \tag{6}$$

The zeros $\{z_n\}$ of $\psi(\phi, \ell)$, or equivalently those of its holomorphic part $\tilde{\psi}(z)$, constitute the Majorana constellation on the cylinder and they uniquely determine the state. Note though that the states $|\psi\rangle$ and $e^{\frac{1}{2}\vartheta\hat{L}^2}\, \hat{E}^k\, e^{-\frac{1}{2}\vartheta\hat{L}^2}\, |\psi\rangle$, with $k \in \mathbb{Z}$, have the same zeros, as a simple calculation shows. According to Cauchy's argument principle [78], the number r_ψ of these zeros inside a simple closed contour C, counted with multiplicity, is

$$r_\psi = \frac{1}{2i\pi} \oint_C \frac{\partial_z \tilde{\psi}(z)}{\tilde{\psi}(z)} dz. \tag{7}$$

Since $\tilde{\psi}(z)/e^{\ln^2|z|}$ is of order zero, the Hadamard factorization theorem [78] ensures that $\tilde{\psi}(z) = \prod_{n=0}^{r_\psi} (z - z_n)$. This number r_ψ is called the stellar rank and has been recently used [79] to establish a hierarchy of non-Gaussian continuous-variable states. The stellar rank of an OAM state can be finite or infinite. For continuous variables, Gaussian states have null rank (i.e., no zeros), according to the famous Hudson theorem [80], yet this theorem does not apply to the cylinder [81].

Examples. We can now illustrate the Majorana constellations for some relevant examples. The two simplest ones are the OAM eigenstate $|\ell_0\rangle$ and the angle eigenstate $|\phi_0\rangle$, with

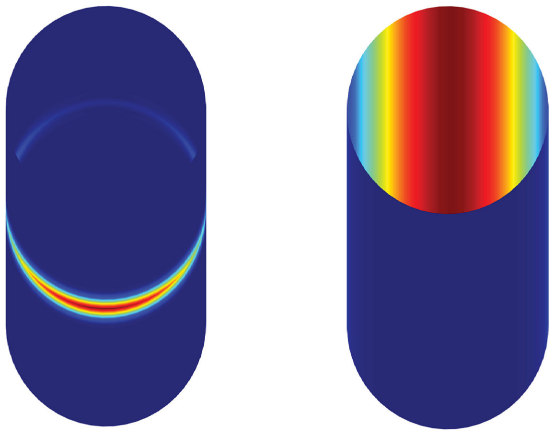

FIG. 1. Husimi distributions for an OAM eigenstate $|\ell_0\rangle$ (with $\ell_0 = 1$) (left) and for an angle eigenstate $|\phi_0\rangle$ (with $\phi_0 = \pi$) (right), represented as a density plot on a continuous cylinder. In both cases, the Q function is positive, so the respective constellations have null stellar rank.

representations

$$\psi_{\ell_0}(\phi,\ell) = \frac{1}{\sqrt{\varpi}} e^{-\frac{1}{2}(\ell-\ell_0)^2} e^{i\ell\phi},$$
$$\psi_{\phi_0}(\phi,\ell) = \frac{1}{\sqrt{2\pi\varpi}} e^{i\ell(\phi-\phi_0)}\, \vartheta_3\left(\frac{1}{2}(\phi-\phi_0)\middle| e^{-\frac{1}{2}}\right), \qquad (8)$$

with $\vartheta_3(u|q) = \sum_{n\in\mathbb{Z}} q^{n^2} e^{-2inu}$ being the third Jacobi theta function [82,83]. Both Husimi distributions are plotted in Fig. 1. For $|\ell_0\rangle$ it consists of rings centered at ℓ_0 and is strictly positive, which agrees with the idea that these are the only states with a positive Wigner function [81]. Similarly, for $|\phi_0\rangle$ the Husimi distribution has no zeros for real phases. This seems to suggest that classical states are those of rank zero, much the same as it happens for continuous variables [79].

For the coherent state $|\phi_0,\ell_0\rangle$, we have now

$$\psi_{\phi_0,\ell_0}(\phi,\ell) = \frac{1}{\varpi} e^{-\frac{1}{2}(\ell^2+\ell_0^2)} \times \vartheta_3\left(\frac{1}{2}(\phi_0-\phi) + \frac{1}{2} i(\ell+\ell_0)\middle| e^{-1}\right). \qquad (9)$$

Surprisingly, this function has infinite zeros located at the angle $\phi - \phi_0 = \pi$ and $\ell + \ell_0 = 2k + 1$ ($k \in \mathbb{Z}$), as we can appreciate in Fig. 2.

We also consider the superposition of OAM eigenstates $|\psi_\pm\rangle = \frac{1}{\sqrt{2}}(|\ell_0\rangle \pm |-\ell_0\rangle)$. For the positive sign we have

$$\psi_+(\phi,\ell) = \frac{1}{\sqrt{2\varpi}} e^{-\frac{1}{2}(\ell^2+\ell_0^2)} \cosh(\ell_0\ell)\, e^{i\ell\phi}, \qquad (10)$$

and an analogous result for the minus sign, but with $\sinh(\ell_0\ell)$. Now, $\psi_+(\phi,\ell)$ has no zeros, whereas $\psi_-(\phi,\ell)$ has one zero at $\ell = 0$.

Finally, we consider catlike states in the cylinder, that is, $|\psi\rangle = (|\phi_0,\ell_0\rangle \pm |\phi_0,\ell_0+\pi\rangle)/\sqrt{\mathcal{N}_0}$, where $\mathcal{N}_0$ is an unessential normalization constant that can be expressed using the second Jacobi theta function $\vartheta_2(u|q) = \sum_{n\in\mathbb{Z}} q^{(n+1/2)^2} e^{(2n+1)iu}$. The resulting stellar representation

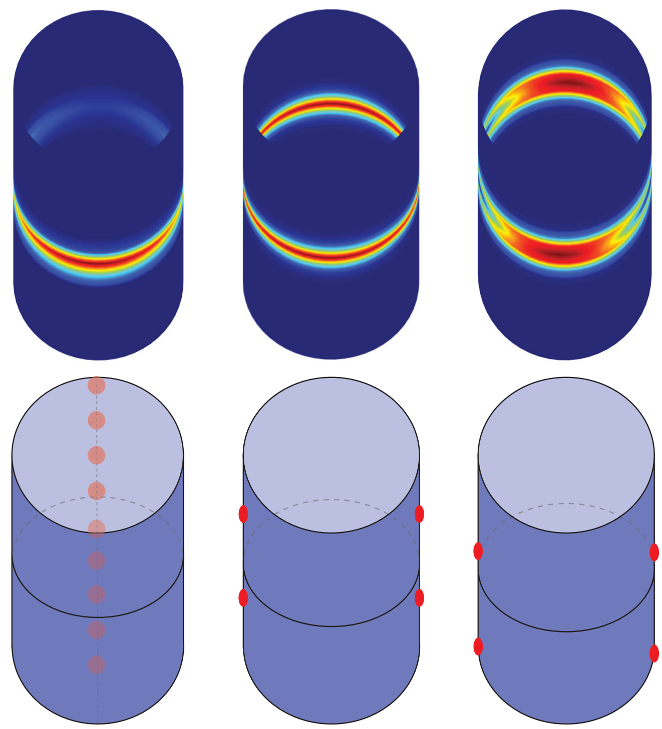

FIG. 2. Density plots of the Husimi distribution (upper panel) and associated constellations on the cylinder (lower panel) for (from left to right) a coherent state $|\phi_0,\ell_0\rangle$ (with $\ell_0 = 1$ and $\phi_0 = 0$), an odd cat, and an even cat (both with $\ell = 1$ and $\phi_0 = 0$). The zeros are calculated in the text and are marked as red points.

reads

$$\psi_{\mathrm{cat}+}(\phi,\ell) = \frac{2}{\varpi\sqrt{\mathcal{N}_0}} e^{-\frac{1}{2}(\ell^2+\ell_0^2)} \times \vartheta_3((\phi_0-\phi) + i(\ell+\ell_0)|e^{-4}),$$
$$\psi_{\mathrm{cat}-}(\phi,\ell) = \frac{2}{\varpi\sqrt{\mathcal{N}_0}} e^{-\frac{1}{2}(\ell^2+\ell_0^2)} \times \vartheta_2((\phi-\phi_0) - i(\ell+\ell_0)|e^{-4}). \qquad (11)$$

Using the properties of these functions, one immediately can see that these functions have two series of zeros at angles $\phi - \phi_0 = \pi/2$ and $\phi - \phi_0 = 3\pi/2$ and $\ell + \ell_0 = 4k - 2$ (for $\psi_{\mathrm{cat}+}$) and $\ell + \ell_0 = 4k$ (for $\psi_{\mathrm{cat}-}$). In Fig. 2, we plot the corresponding constellations for these states.

Multipole expansion. The Majorana constellation introduced thus far provides an intriguing and useful visualization of OAM states. Nevertheless, to assess their quantumness it would be convenient to have a more quantitative measure. For the archetypal case of SU(2), the multipole expansion is the proper tool [84]. Apart from their good transformation properties [85], multipoles can be understood as the coefficients of the expansion of the Husimi distribution in the spherical harmonics [15], which constitute an orthonormal basis of functions on the sphere.

To extend this notion to the cylinder, one has to find a proper basis on X. It is easy to check that the set $\mathfrak{e}_{nk}(\phi,\ell) = \delta_{\ell k} e^{in\phi}$ plays for our problem the same role as the spherical harmonics for SU(2). In consequence, we can define the

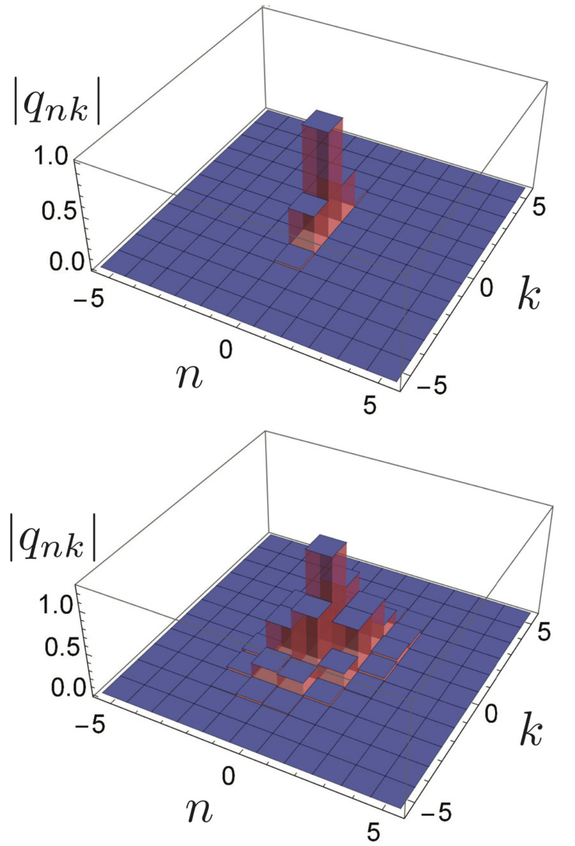

FIG. 3. Multipole distribution $|q_{nk}|$ for the OAM eigenstate (with $\ell_0 = 1$) (left) and a coherent state (with $\phi_0 = 0$, $\ell_0 = 1$) (right).

multipoles as

$$
\begin{aligned}
q_{nk} &= \frac{1}{2\pi} \sum_{\ell \in \mathbb{Z}} \int_0^{2\pi} Q(\phi, \ell) \mathfrak{e}_{nk}(\phi, \ell) d\phi \\
&= \frac{1}{2\pi} \int_0^{2\pi} Q(\phi, k) e^{in\phi} d\phi.
\end{aligned} \tag{12}
$$

They can be experimentally determined [86] as moments of the Husimi distribution and contain complete information about the state, as we have the inverse expansion $Q(\phi, \ell) = \sum_{n,k} q_{nk} \mathfrak{e}^*_{nk}(\phi, \ell)$. Actually, one can straightforwardly compute these multipoles for the previous states. For the OAM eigenstate, $|\psi\rangle = |\ell_0\rangle$, we find $q_{nk} \propto e^{-(k-\ell_0)^2} \delta_{n0}$: This a very peaked distribution around the first moment $n = 0$. These states, as commented before [81], the only ones with a non-negative Wigner function, play the role of Clifford states and can thus be efficiently simulated by a classical computer [87]. This seems to confirm previous results that point out that for classical states the first multipoles contribute the most.

Interestingly, for a coherent state, the multipole distribution, as plotted in Fig. 3, is much more spread, and so most quantum. The status of coherent states for the cylinder is thus drastically different from that of continuous variables, where they are the most classical states.

Dynamics of the constellations. It is interesting to check how the constellation evolves in time for the typical states considered before. We take as the interaction Hamiltonian

$$
\hat{H} = \lambda \cos(\hat{\phi}) = \tfrac{1}{2} \lambda (\hat{E} + \hat{E}^\dagger), \tag{13}
$$

with $\hat{\phi}$ the angle operator and λ a coupling constant. This model can represent a variety of situations, such as the dynamics of a discrete-time quantum walk [88] or the tunneling in a Josephson junction [89], where in such a case, λ is the Josephson energy and the conjugate operator $\hat{L}$ corresponds to the number of excess Cooper pairs in the island.

At time t the evolved wave function $|\psi(t)\rangle = \exp(i\hat{H}t)\,|\psi\rangle$ can be written in the OAM basis as [90]

$$
|\psi(t)\rangle = \sum_{\ell, \ell' \in \mathbb{Z}} \psi_{\ell'} i^{\ell} J_\ell(\lambda t)\, |\ell + \ell'\rangle\,, \tag{14}
$$

where J_ℓ are Bessel functions of the first kind and order ℓ. In consequence, the stellar representation after the dynamics turns to be

$$
\psi(\phi, \ell; t) = \frac{1}{\sqrt{\varpi}} e^{-\frac{1}{2}\ell^2} \sum_{\ell' \in \mathbb{Z}} \psi_{\ell'}(t) e^{-\frac{1}{2}\ell'^2} e^{\ell' z}, \tag{15}
$$

with $\psi_\ell(t) = \sum_{\ell' \in \mathbb{Z}} \psi_{\ell'} i^{\ell' - \ell} J_{\ell' - \ell}(\lambda t)$.

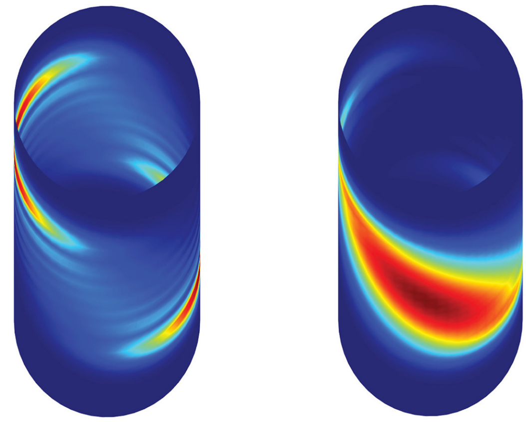

FIG. 4. Density plots of the Husimi distribution of an OAM eigenstate $|\ell_0\rangle$ (with $\ell_0 = 1$) (left) and a coherent state (with $\phi_0 = 0$ and $\ell_0 = 1$) (right), after evolution with the dynamics given in (15) at time $\lambda t = 10$.

In Fig. 4, we represent the resulting stellar distribution for the OAM eigenstate $|\ell_0\rangle$ and the coherent state $|\phi_0, \ell_0\rangle$ at $\lambda t = 10$.

Concluding remarks. In summary, we have advocated the use of the discrete cylinder to properly represent OAM states and their dynamics. In this vein, we have introduced a *bona fide* Majorana representation on the cylinder and we have illustrated its behavior with various examples of significant states. The resulting constellations translate the symmetry of the states in a natural and crystal-clear way.

In the Bloch sphere, constellations having their points arranged as symmetrically as possible are the most quantum, whereas the opposite occurs for coherent states. One might argue that the same holds true for twisted photons: The distribution of the zeros is an indicator of quantumness. Moreover, for the sphere, the "Kings of Quantumness" [13] have nice extremal properties, including an amazing metrological power. Since tailoring the Majorana constellation is feasible in the laboratory, one should explore the potential of these extremal states for the cylinder; work along these lines is in progress.

Acknowledgments. We acknowledge discussions with A. Z. Goldberg and P. de la Hoz. This work received funding from the Spanish Ministerio de Ciencia e Innovación (Grant No. PID2021-127781NB-I00).

[1] E. Majorana, Atomi orientati in campo magnetico variabile, Nuovo Cimento **9**, 43 (1932).

[2] H. Mäkelä and A. Messina, n-qubit states as points on the Bloch sphere, Phys. Scr. **2010**, 014054 (2010).

[3] A. R. U. Devi, Sudha, and A. K. Rajagopal, Majorana representation of symmetric multiqubit states, Quantum Inf. Process. **11**, 685 (2012).

[4] C. Yang, H. Guo, L.-B. Fu, and S. Chen, Characterization of symmetry-protected topological phases in polymerized models by trajectories of Majorana stars, Phys. Rev. B **91**, 125132 (2015).

[5] Y.-G. Su, F. Yao, H.-B. Liang, Y.-M. Che, L.-B. Fu, and X.-G. Wang, Majorana stellar representation for mixed-spin $(s, 1/2)$ systems, Chin. Phys. B **30**, 030303 (2021).

[6] P. Ribeiro, J. Vidal, and R. Mosseri, Thermodynamical Limit of the Lipkin-Meshkov-Glick Model, Phys. Rev. Lett. **99**, 050402 (2007).

[7] P. Ribeiro and R. Mosseri, Entanglement in the Symmetric Sector of n Qubits, Phys. Rev. Lett. **106**, 180502 (2011).

[8] H. D. Liu and L. B. Fu, Berry phase and quantum entanglement in Majorana's stellar representation, Phys. Rev. A **94**, 022123 (2016).

[9] A. Lamacraft, Low-energy dynamics of spinor condensates, Phys. Rev. B **81**, 184526 (2010).

[10] B. Lian, T.-L. Ho, and H. Zhai, Searching for non-Abelian phases in the Bose-Einstein condensate of dysprosium, Phys. Rev. A **85**, 051606(R) (2012).

[11] X. Cui, B. Lian, T. L. Ho, B. L. Lev, and H. Zhai, Synthetic gauge field with highly magnetic lanthanide atoms, Phys. Rev. A **88**, 011601(R) (2013).

[12] J. H. Hannay, The Majorana representation of polarization, and the Berry phase of light, J. Mod. Opt. **45**, 1001 (1998).

[13] G. Björk, A. B. Klimov, P. de la Hoz, M. Grassl, G. Leuchs, and L. L. Sánchez-Soto, Extremal quantum states and their Majorana constellations, Phys. Rev. A **92**, 031801(R) (2015).

[14] G. Björk, M. Grassl, P. de la Hoz, G. Leuchs, and L. L. Sánchez-Soto, Stars of the quantum universe: extremal constellations on the Poincaré sphere, Phys. Scr. **90**, 108008 (2015).

[15] A. Z. Goldberg, P. de la Hoz, G. Björk, A. B. Klimov, M. Grassl, G. Leuchs, and L. L. Sánchez-Soto, Quantum concepts in optical polarization, Adv. Opt. Photonics **13**, 1 (2021).

[16] R. Gutiérrez-Cuevas, S. A. Wadood, A. N. Vamivakas, and M. A. Alonso, Modal Majorana Sphere and Hidden Symmetries of Structured-Gaussian Beams, Phys. Rev. Lett. **125**, 123903 (2020).

[17] R. Gutiérrez-Cuevas and M. A. Alonso, Platonic Gaussian beams: wave and ray treatment, Opt. Lett. **45**, 6759 (2020).

[18] C. Chryssomalakos and H. Hernández-Coronado, Optimal quantum rotosensors, Phys. Rev. A **95**, 052125 (2017).

[19] F. Bouchard, P. de la Hoz, G. Bjork, R. W. Boyd, M. Grassl, Z. Hradil, E. Karimi, A. B. Klimov, G. Leuchs, J. Rehacek, and L. L. Sanchez-Soto, Quantum metrology at the limit with extremal Majorana constellations, Optica **4**, 1429 (2017).

[20] A. Z. Goldberg and D. F. V. James, Quantum-limited Euler angle measurements using anticoherent states, Phys. Rev. A **98**, 032113 (2018).

[21] A. Z. Goldberg, A. B. Klimov, G. Leuchs, and L. L. Sánchez-Soto, Rotation sensing at the ultimate limit, J. Phys.: Photonics **3**, 022008 (2021).

[22] J. H. Hannay, The Berry phase for spin in the Majorana representation, J. Phys. A: Math. Gen. **31**, L53 (1998).

[23] P. Bruno, Quantum Geometric Phase in Majorana's Stellar Representation: Mapping onto a Many-Body Aharonov-Bohm Phase, Phys. Rev. Lett. **108**, 240402 (2012).

[24] C. Chryssomalakos, E. Guzmán-González, and E. Serrano-Ensástiga, Geometry of spin coherent states, J. Phys. A: Math. Theor. **51**, 165202 (2018).

[25] X. Gao, M. Erhard, A. Zeilinger, and M. Krenn, Computer-Inspired Concept for High-Dimensional Multipartite Quantum Gates, Phys. Rev. Lett. **125**, 050501 (2020).

[26] H.-H. Lu, Z. Hu, M. S. Alshaykh, A. J. Moore, Y. Wang, P. Imany, A. M. Weiner, and S. Kais, Quantum phase estimation with time-frequency qudits in a single photon, Adv. Quantum Technol. **3**, 1900074 (2020).

[27] S. D. Bartlett, H. de Guise, and B. C. Sanders, Quantum encodings in spin systems and harmonic oscillators, Phys. Rev. A **65**, 052316 (2002).

[28] M. R. A. Adcock, P. Høyer, and B. C. Sanders, Quantum computation with coherent spin states and the close Hadamard problem, Quantum Inf. Process. **15**, 1361 (2016).

[29] A. B. Klimov, R. Guzmán, J. C. Retamal, and C. Saavedra, Qutrit quantum computer with trapped ions, Phys. Rev. A **67**, 062313 (2003).

[30] Z. Gedik, I. A. Silva, B. Çakmak, G. Karpat, E. L. G. Vidoto, D. O. Soares-Pinto, E. R. de Azevedo, and F. F. Fanchini, Computational speed-up with a single qudit, Sci. Rep. **5**, 14671 (2015).

[31] M. N. Leuenberger and D. Loss, Quantum computing in molecular magnets, Nature (London) **410**, 789 (2001).

[32] M. Erhard, R. Fickler, M. Krenn, and A. Zeilinger, Twisted photons: New quantum perspectives in high dimensions, Light: Sci. Appl. **7**, 17146 (2018).

[33] H. Bechmann-Pasquinucci and A. Peres, Quantum Cryptography with 3-State Systems, Phys. Rev. Lett. **85**, 3313 (2000).

[34] D. Bruß and C. Macchiavello, Optimal Eavesdropping in Cryptography with Three-Dimensional Quantum States, Phys. Rev. Lett. **88**, 127901 (2002).

[35] Y. Wang, Z. Hu, B. C. Sanders, and S. Kais, Qudits and high-dimensional quantum computing, Front. Phys. **8**, 589504 (2020).

[36] D. Kaszlikowski, P. Gnaciński, M. Żukowski, W. Miklaszewski, and A. Zeilinger, Violations of Local Realism by Two

Entangled N-Dimensional Systems Are Stronger than for Two Qubits, Phys. Rev. Lett. **85**, 4418 (2000).

[37] D. Collins, N. Gisin, N. Linden, S. Massar, and S. Popescu, Bell Inequalities for Arbitrarily High-Dimensional Systems, Phys. Rev. Lett. **88**, 040404 (2002).

[38] T. Vértesi, S. Pironio, and N. Brunner, Closing the Detection Loophole in Bell Experiments Using Qudits, Phys. Rev. Lett. **104**, 060401 (2010).

[39] N. Bent, H. Qassim, A. A. Tahir, D. Sych, G. Leuchs, L. L. Sánchez-Soto, E. Karimi, and R. W. Boyd, Experimental Realization of Quantum Tomography of Photonic Qudits via Symmetric Informationally Complete Positive Operator-Valued Measures, Phys. Rev. X **5**, 041006 (2015).

[40] P. Carruthers and M. M. Nieto, Phase and angle variables in quantum mechanics, Rev. Mod. Phys. **40**, 411 (1968).

[41] S. D. Augustin and H. Rabitz, Action-angle variables in quantum mechanics, J. Chem. Phys. **71**, 4956 (1979).

[42] R. Lynch, The quantum phase problem: A critical review, Phys. Rep. **256**, 367 (1995).

[43] V. Peřinova, A. Lukš, and J. Peřina, *Phase in Optics* (World Scientific, Singapore, 1998).

[44] A. Luis and L. L. Sánchez-Soto, Quantum phase difference, phase measurements and quantum Stokes parameters, Prog. Opt. **41**, 421 (2000).

[45] S. M. Barnett and D. T. Pegg, Quantum theory of rotation angles, Phys. Rev. A **41**, 3427 (1990).

[46] A. Luis and L. L. Sánchez-Soto, Quantum theory of rotation angles: The problem of angle sum and angle difference, Eur. Phys. J. D **3**, 195 (1998).

[47] J. P. Gazeau and F. H. Szafraniec, Three paths toward the quantum angle operator, Ann. Phys. **375**, 16 (2016).

[48] P. Kasperkovitz and M. Peev, Wigner-Weyl formalisms for toroidal geometries, Ann. Phys. **230**, 21 (1994).

[49] J. F. Plebański, M. Przanowski, J. Tosiek, and F. J. Turrubiates, Remarks on deformation quantization on the cylinder, Acta Phys. Pol. B **31**, 561 (2000).

[50] J. González, M. A. del Olmo, and J. Tosiek, Quantum mechanics on the cylinder, J. Opt. B: Quantum Semiclass. Opt. **5**, S306 (2003).

[51] N. Mukunda, Wigner distribution for angle coordinates in quantum mechanics, Am. J. Phys. **47**, 182 (1979).

[52] M. Ruzzi and D. Galetti, Schwinger and Pegg–Barnett approaches and a relationship between angular and Cartesian quantum descriptions: II. Phase spaces, J. Phys. A: Math. Gen. **35**, 4633 (2002).

[53] N. Mukunda, G. Marmo, A. Zampini, S. Chaturvedi, and R. Simon, Wigner–Weyl isomorphism for quantum mechanics on Lie groups, J. Math. Phys. **46**, 012106 (2005).

[54] H. A. Kastrup, Wigner functions for the pair angle and orbital angular momentum, Phys. Rev. A **94**, 062113 (2016).

[55] K. Kowalski and K. Ławniczak, Wigner functions and coherent states for the quantum mechanics on a circle, J. Phys. A: Math. Theor. **54**, 275302 (2021).

[56] K. Kowalski, J. Rembieliński, and L. C. Papaloucas, Coherent states for a quantum particle on a circle, J. Phys. A: Math. Gen. **29**, 4149 (1996).

[57] J. A. González and M. A. del Olmo, Coherent states on the circle, J. Phys. A: Math. Gen. **31**, 8841 (1998).

[58] Y. Ohnuki and S. Kitakado, Fundamental algebra for quantum mechanics on S^D and gauge potentials, J. Math. Phys. **34**, 2827 (1993).

[59] B. C. Hall and J. J. Mitchell, Coherent states on spheres, J. Math. Phys. **43**, 1211 (2002).

[60] M. Ruzzi, M. A. Marchiolli, E. C. da Silva, and D. Galetti, Quasiprobability distribution functions for periodic phase spaces: I. Theoretical aspects, J. Phys. A: Math. Gen. **39**, 9881 (2006).

[61] H. A. Kastrup, Quantization of the canonically conjugate pair angle and orbital angular momentum, Phys. Rev. A **73**, 052104 (2006).

[62] I. Rigas, L. L. Sanchez-Soto, A. B. Klimov, J. Rehacek, and Z. Hradil, Orbital angular momentum in phase space, Ann. Phys. **326**, 426 (2011).

[63] H. Bacry, *Group Theory and Constellations* (Publibook, Paris, 2004).

[64] I. Bengtsson and K. Życzkowski, *Geometry of Quantum States* (Cambridge University Press, Cambridge, UK, 2017).

[65] A. Z. Goldberg, A. B. Klimov, M. Grassl, G. Leuchs, and L. L. Sánchez-Soto, Extremal quantum states, AVS Quantum Sci. **2**, 044701 (2020).

[66] E. C. Lerner, Harmonic-oscillator phase operators, Nuovo Cimento B **56**, 183 (1968).

[67] Z. Hradil, J. Řeháček, Z. Bouchal, R. Čelechovský, and L. L. Sánchez-Soto, Minimum Uncertainty Measurements of Angle and Angular Momentum, Phys. Rev. Lett. **97**, 243601 (2006).

[68] J. E. Humphreys, *Introduction to Lie Algebras and Representation Theory* (Springer, New York, 1972).

[69] A. Perelomov, *Generalized Coherent States and their Applications* (Springer, Berlin, 1986).

[70] A. O. Barut and L. Girardello, New "coherent" states associated with non-compact groups, Commun. Math. Phys. **21**, 41 (1971).

[71] J.-P. Gazeau and R. Murenzi, Integral quantization for the discrete cylinder, Quantum Rep. **4**, 362 (2022).

[72] J.-P. Gazeau, *Coherent States in Quantum Physics* (Wiley, New York, 2009), p. 360.

[73] P. Dirichlet, Sur la convergence des séries trigonometriques qui servent à représenter une fonction arbitraire entre des limites données, J. Math. **1829**, 157 (1829).

[74] L. Fejér, Untersuchungen über Fouriersche Reihen, Math. Ann. **58**, 51 (1904).

[75] L. Mišta, H. de Guise, J. Řeháček, and Z. Hradil, Angle and angular momentum: Uncertainty relations, simultaneous measurement, and phase-space representation, Phys. Rev. A **106**, 022204 (2022).

[76] K. Husimi, Some formal properties of the density matrix, Proc. Phys. Math. Soc. Jpn. **22**, 264 (1940).

[77] I. Nape, B. Sephton, P. Ornelas, C. Moodley, and A. Forbes, Quantum structured light in high dimensions, APL Photonics **8**, 051101 (2023).

[78] W. Rudin, *Real and Complex Analysis* (McGraw-Hill, New York, 1986).

[79] U. Chabaud, D. Markham, and F. Grosshans, Stellar Representation of Non-Gaussian Quantum States, Phys. Rev. Lett. **124**, 063605 (2020).

[80] R. L. Hudson, When is the Wigner quasi-probability density non-negative? Rep. Math. Phys. **6**, 249 (1974).

[81] I. Rigas, L. L. Sánchez-Soto, A. B. Klimov, J. Řeháček, and Z. Hradil, Non-negative Wigner functions for orbital angular momentum states, Phys. Rev. A **81**, 012101 (2010).
[82] D. Mumford, *Tata Lectures on Theta I* (Birkhauser, Boston, 1983).
[83] DLMF, *NIST Digital Library of Mathematical Functions*, edited by F. W. J. Olver, A. B. Olde Daalhuis, D. W. Lozier, B. I. Schneider, R. F. Boisvert, C. W. Clark, B. R. Miller, B. V. Saunders, H. S. Cohl, and M. A. McClain, http://dlmf.nist.gov/, Release 1.1.8 of 2022-12-15.
[84] K. Blum, *Density Matrix Theory and Applications* (Plenum, New York, 1981).
[85] U. Fano and G. Racah, *Irreducible Tensorial Sets* (Academic, New York, 1959).
[86] A. Z. Goldberg, A. B. Klimov, H. de Guise, G. Leuchs, G. S. Agarwal, and L. L. Sánchez-Soto, From polarization multipoles to higher-order coherences, Opt. Lett. **47**, 477 (2022).
[87] S. Aaronson and D. Gottesman, Improved simulation of stabilizer circuits, Phys. Rev. A **70**, 052328 (2004).
[88] F. Cardano, F. Massa, H. Qassim, E. Karimi, S. Slussarenko, D. Paparo, C. de Lisio, F. Sciarrino, E. Santamato, R. W. Boyd, and L. Marrucci, Quantum walks and wavepacket dynamics on a lattice with twisted photons, Sci. Adv. **1**, e1500087 (2015).
[89] Y. A. Pashkin, O. Astafiev, T. Yamamoto, Y. Nakamura, and J. S. Tsai, Josephson charge qubits: A brief review, Quantum Inf. Process. **8**, 55 (2009).
[90] L. M. Nieto, N. M. Atakishiyev, S. M. Chumakov, and K. B. Wolf, Wigner distribution function for Euclidean systems, J. Phys. A: Math. Gen. **31**, 3875 (1998).